Mechanical and Thermal Performances of Rubber/Graphite Derivatives: Facile Synthesis, Characterization, and Formulation

Jawhid, Omid; Zohuri, Gholam Hossein*[+•]

Department of Chemistry, Faculty of Science, Ferdowsi University of Mashhad, Mashhad, I.R. IRAN

Nourmohammadi, Mohammad

Department of Research and Development, Ayegh Khodro Toos (AKT) Co. of Part Lastic Industry Group, P.O. Box 91851-77209 Mashhad, I.R. IRAN

ABSTRACT: *A larger scale production of Graphene Oxide (GO), reduced graphene oxide (rGO), and reduced GO decorated with SiO_2 (rGO@SiO_2) as graphite-derivatives are reported. The pristine graphite (Gt), synthesized rGO, and rGO@SiO_2 were dispersed in dioctyl phthalate (DOP) assisted using the sonication technique. Styrene Butadiene Rubber (SBR)-based elastomer was first formulated and the homogenized samples are loaded into the SBR polymer matrix using a Bunbury-type kneader. Common industrial-grade materials were used to synthesize additives and compound formulations, and loading the additives into the polymer was mechanically performed. From an economic point of view, it means this product could be easily commercialized. Fourier-Transform InfraRed (FT-IR) spectroscopy spectrum index bands of prepared GO and rGO@SiO_2 appeared at about 1725 and 1064 cm^{-1}, respectively. X-Ray Diffraction (XRD) was used to study the crystal structure of the synthesized materials. The surface morphology of the synthesized materials and separation of pristine graphite compressed layers were verified with Transmission Electron Microscopy (TEM) images. Mechanical tests of the compounded products showed good tensile stress, and virtually two folds greater than blank rubber. Thermogravimetric analyses investigation showed that a clear improvement of thermal stability of composites increased with adding the synthesized carbon-based additives. The prepared rGO/SBR and rGO@SiO_2/SBR composites exhibited higher oxidative-induction times (13.84 and 9.39 min, respectively) compared with the blank SBR compound.*

KEYWORDS*: Graphite-derivatives synthesis; Compound formulation; Composite; Thermal stability; Tensile stress.*

INTRODUCTION

During the last few decades, many novel polymer nanocomposites with enhanced thermal, electrical and mechanical properties have been investigated and applied to meet the demand [1-5]. The most commonly used

***** *To whom correspondence should be addressed.*

+ E-mail: zohuri@um.ac.ir

• Other Address: Environmental Chemistry Research Centre. Department of Chemistry, Faculty of Science, Ferdowsi University of Mashhad, Mashhad, I.R. IRAN

1021-9986/2022/4/1240-1249 10/$/6.00

approach to making polymers with mentioned properties is the incorporation of nano-additives in the polymer matrix. This method is generally preferred over the others because it is easily compatible with industrial processes and it offers a good compromise between economic considerations, mechanical, thermal, and other special properties [6-10]. Carbon-based nano-additives, such as Carbon Nano Tube (CNT) and graphite derivatives, owing to their intrinsic specific properties, were considered an ideal material, which can simultaneously improve both the thermal stability and mechanical strength of polymers [11-13].

Among polymeric materials, elastomer-type polymers are famous for their easy processing, crack resistance, and high flexibility [14, 15]. Styrene-butadiene rubber is one of the nonpolar and cheap synthetic elastomers with a general purpose that is widely used as one of the components of the elastomeric matrix for automotive tires [16, 17], as well as for wire and cable applications [18] which can be used as a commercial matrix for rubber nanocomposite fabrication [19-21].

Introducing of ceramic fillers, such as Boron Nitride (BN) [22-24], Aluminum Nitride (AlN) [25], aluminum oxide (Al_2O_3) [26, 27], zinc oxide (ZnO) [28, 29], silicon carbide (SiC) [30, 31] and carbon-based materials [32-34], into a polymer matrix have attracted more attention in order to improve their thermal conductivity and electrical insulating properties. In general, nitrides may provide many better-desired attributes in comparison with oxides, they are, however, also more expensive than oxides [35]. Graphene nanosheets and their derivatives exhibit superior mechanical, thermal, and electrical properties to elastomeric polymers [36-38]. The unique properties of graphene arise from 2-dimensional (2D) sheet-like chemical structure. Due to the covalently strong bonded of each carbon to three other carbon atoms, graphene nano-layers show great stability and very high tensile strength. The dense packing of atoms and the strong chemical bonds between them causes the rapid transmission of vibrations between the neighboring atoms in a layer [39-41]. Coating of electrically insulating layers onto carbon-based materials has been widely developed, for example, Al_2O_3@rGO [42], rGO@SiO_2 [43, 44], and SiC@GO [45]. Although these kinds of surface modifications of graphene increase the thickness of layers due to the association of organic molecules, they would prevent agglomeration of the layers [46].

In this study, few-layer GO was synthesized from commercially grade graphite flakes using a modified Hummers method. The prepared GO layers were chemically surface-modified to synthesize rGO@SiO_2. A simple one-step process was applied to prepare reduced graphene oxide (Fig. 1). The synthesized graphite-based derivatives were used separately as an additive to improve the thermal and mechanical properties of SBR elastomer.

EXPERIMENTAL SECTION

Materials

Hydrochloric acid (37%) and $KMnO_4$ came from Dr. Mojallali Co. Ltd (Iran). Sulfuric acid (98.5 %) and phosphoric acid (48-54 %) were received from Razi Petrochemical Company (RPC, Iran). Ethanol (96%), tetraethyl orthosilicate (TEOS), and hydrogen peroxide (30%) were provided from Merck Co. Ltd. Styrene-butadiene rubber (SBR-1502, with styrene content 22.5-24.5 wt%) received from Bandar Imam Petrochemical Company (BIPC, Iran). Other reagents were all analytical-grade and commercially available. Deionized water was used throughout the whole work.

Preparation of GO

GO was prepared from commercially grade graphite flake *via* a modified Hummer's method. Gt (30 g) was dispersed in a mixture of phosphoric acid (50 mL) and sulfuric acid (450 mL) using continuous stirring at room temperature for 3 h. The mixture was cooled down (to 5 ℃) in an ice bath, and potassium permanganate (90 g) was very slowly added so that the temperature does not increase from 10 ℃. The mixture was stirred for 2 h (at lower than 20 ℃). The reaction mixture was stirred for a further 2 h (at 50 ℃) and then cooled using an ice bath to 5 ℃. Ice water (450 mL) was slowly added to the reaction mixture maintaining the temperature at 50 ℃ or less. H_2O_2 (30 wt.%) was then slowly mixed into the reaction until the bubbling has stopped completely. The brown colored product was filtrated, washed with HCl (10%, 3 times) followed with water (5 times), and was then freeze-dried (at -50 ℃ for 24 h) [47, 48].

Synthesis of reduced graphene oxide (rGO)

The reduced graphene oxide was prepared using a modified approach [49]. In a typical procedure, graphite

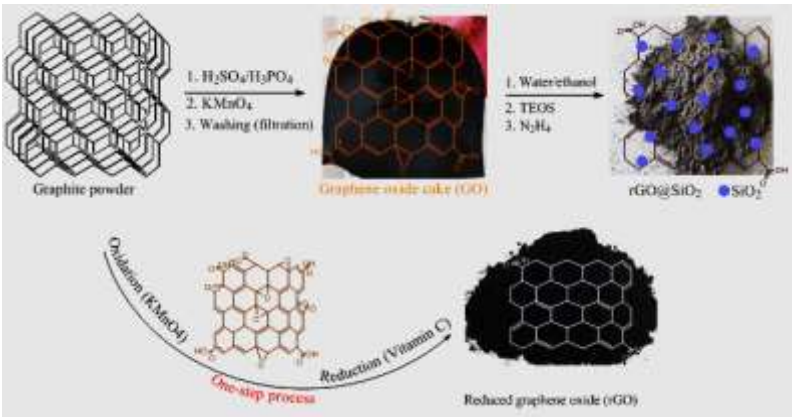

Fig. 1: Schematic presentation of synthesis of GO, rGO@SiO_2, and rGO.

flakes (20 g) were dispersed in a mix of phosphoric acid (39 mL) and sulfuric acid (300 mL) in an ice-water bath (at 0-5 °C, for 50 min). Potassium permanganate (60 g) was slowly added by maintaining the temperature under 12 °C. The reaction was carried out at 50 °C under a mechanical-mixing process (until the reaction color changes from dark green to brown, 1.5 h). Water (100 mL) and sodium hydroxide solution (100 mL, 1 M) were added to the reaction, stirring was carried out for a further 40 min. Ascorbic Acid (AA) powder (100 g) which was dissolved in water (500 mL) was added to the viscose graphite oxide suspension (at room temperature). A dark brown slurry solution was quickly obtained. After maintaining the reaction temperature at about 98-103 °C (for 2 h), exfoliation was started and carried out for 15 min. The resultant black precipitate was washed using HCl and water with vacuum filtration and dried under vacuum at 80 °C.

Preparation of rGO@SiO_2

The prepared GO (20 g) was dispersed in a mixture of the solvent containing water (90 mL) and ethanol (480 mL, 96%) using sonication (30 min) followed by the addition of NH_4OH (40 mL, 25%) under stirring (for 15 min). TEOS (42 mL) was added drop-wise into the solution and sonicated further (for 40 min). After stirring the mixture at room temperature (2 h), hydrazine hydrate (40 mL) was added and refluxed (at 80 ℃ for 12 h). The resulting product was filtrated and washed with water and ethanol several times; oven dried (at 70 ℃ for 24 h) to obtain a chemical called rGO@SiO_2 composite [43].

Formulation of rubber compound

The sequences of rubber compounding were done based on ASTM D3184-80 on a Bunbury-type kneader by the following two steps: master batch preparation (at ~100 ℃) and finally compounding process (at 50-60 ℃).

The preparation of the blank (without synthesized additives) master batch followed by: the raw SBR (with styrene content 22.5-24.5 wt%, 500 g) masticated in the kneader (for 15 min at 100 °C). Plasticizer (DOP), filler ($CaCO_3$), ZnO, and stearic acid (St) were added and mixed (frequency of 125 Hz, for 40 min at 100-108 °C).

The produced master batch was cooled at room temperature, and immersed into the kneader again, followed by adding DOP, sulfur (S), and MBTS, mixed (frequency of 111 Hz, for 20 min at 70 °C) to prepare the final rubber dough. The sheets (10×10×0.5 mm) of the rubber dough were prepared using a two-roll mill and vulcanized in an oven (at 160 °C for 40 min).

All other sheets were prepared in the same process. For better distribution in the SBR chains, the additives (graphite, rGO, and rGO@SiO_2) were dispersed in DOP using the sonication technique (for 30 min) and then added to the elasticated SBR (Table 1).

Characterization

The microstructure and surface morphology of the synthesized materials were studied by Transmission Electron Microscope (TEM, LEO 912 AB, Germany). The chemical structure of the materials at each stage was followed by using FT-IR spectroscopy (Thermo-Nicolet Avatar 370) using a standard KBr pellet technique. X-Ray Diffraction (XRD) analysis was carried out in the room

Table 1: Formula of SBR composites reinforced with graphite and modified graphite layers.

Processing steps	Ingredients	Samples code			
		Blank (phr)	Gt/SBR (phr)	SiO_2@rGO/SBR (phr)	rGO/SBR (phr)
Master batch production process	SBR	100	100	100	100
	DOP	40	40	40	40
	St	2	2	2	2
	Filler ($CaCO_3$)	90	90	90	90
	ZnO	5	5	5	5
	Gt	-	4	-	-
	SiO_2@rGO	-	-	4	-
	rGO	-	-	-	4
Finally processing	S = 3 phr, MBTS = 3 phr, DOP = 10 phr				

temperature from 2θ=5° to 40° at a generator voltage of 40 kV and a generator current of 30 mA with a step size of 0.05° using a GNR EXPLORER (Italy). Thermogravimetric analysis (TGA-50, Shimadzu Co., Japan) was conducted to mass loss percentage measuring of the products, with a heating rate of 10 ℃/min from 100 ℃ to 800 ℃ under an air atmosphere. The Oxidation Induction Time (OIT) of the products was evaluated by a 100-L differential scanning calorimeter (Nanjing Dazhan Institute of Electromechanical Technology, China) according to the standard method (ISO 11357-6, 2008). A testing machine Instron (SANTAM STM-5) with 50 N load cell was used for the investigation of tensile and elongation properties of the final products.

RESULTS AND DISCUSSION

The topography of the synthesized GO layer is shown in Fig. 2. A two-dimensional line profile recorded along the dashed line of Fig. 2d is presented. This height profile of approximately 0.3 nm layer thickness confirms the detection of a single GO sheet as shown in Fig. 2d. This height is similar to single-layer GO sheet heights reported in the previous study [50].

The structure and morphology of the synthesized GO and rGO@SiO_2 surface were investigated using TEM images (Fig. 2). It is clear how the graphite sheets are placed on each other and appear as a large thick dark flake (Fig. 2a).

Fig. 2b shows that the graphene oxide sheets are smooth and exhibited a transparent few-layered structure [51]. In the final product, however, the particles are coated uniformly on the graphene surface and silica layer has been formed (Fig. 2c) [52]. The images prove that after graphite oxidation the number of layers is reduced, crystallinity decreased and amorphization occurs.

Fig.3 shows the FT-IR spectra of pristine material and the synthesized samples. The index bonds of the synthesized GO spectra at 1603, 1225, and 1051 cm^{-1} are assigned to the C=C bending, C-O vibration, and C-O-C stretching, respectively. Stretching vibrations of carbonyl groups observed at 1725 cm^{-1} indicate the formation of carboxyl, quinone, and six-membered lactone moieties after oxidation of graphite. The broad band at ~3300–3400 cm^{-1} attributed to the C–OH stretching vibrations [53]. The analysis of rGO presented two bonds at 3431 and 1570 cm^{-1} corresponding to the stretching and bending vibration of OH groups of water molecules adsorbed on rGO (Fig. 3). Although the graphite oxide had been reduced by hydrazine, the peak at 1110 cm^{-1} corresponds to the stretching vibration of C−OH of alcohol was observed in FT-IR spectrum of rGO. The peaks located at 1064, 1631, and 3428 cm^{-1} in the final product, correspond to the asymmetry stretching mode of Si-O-Si, the bending vibration of H-O-H, and the stretching vibration of -OH, respectively (Fig. 3).

The crystalline structure of graphite and its synthesized derivatives were studied using XRD analysis, as shown in Fig. 4. The X-ray diffractogram for pristine graphite powder (Fig. 4) provided a characteristic peak at 2θ=26° (d_{002}=0.34 nm) related to 002 planes [54]. The diffraction

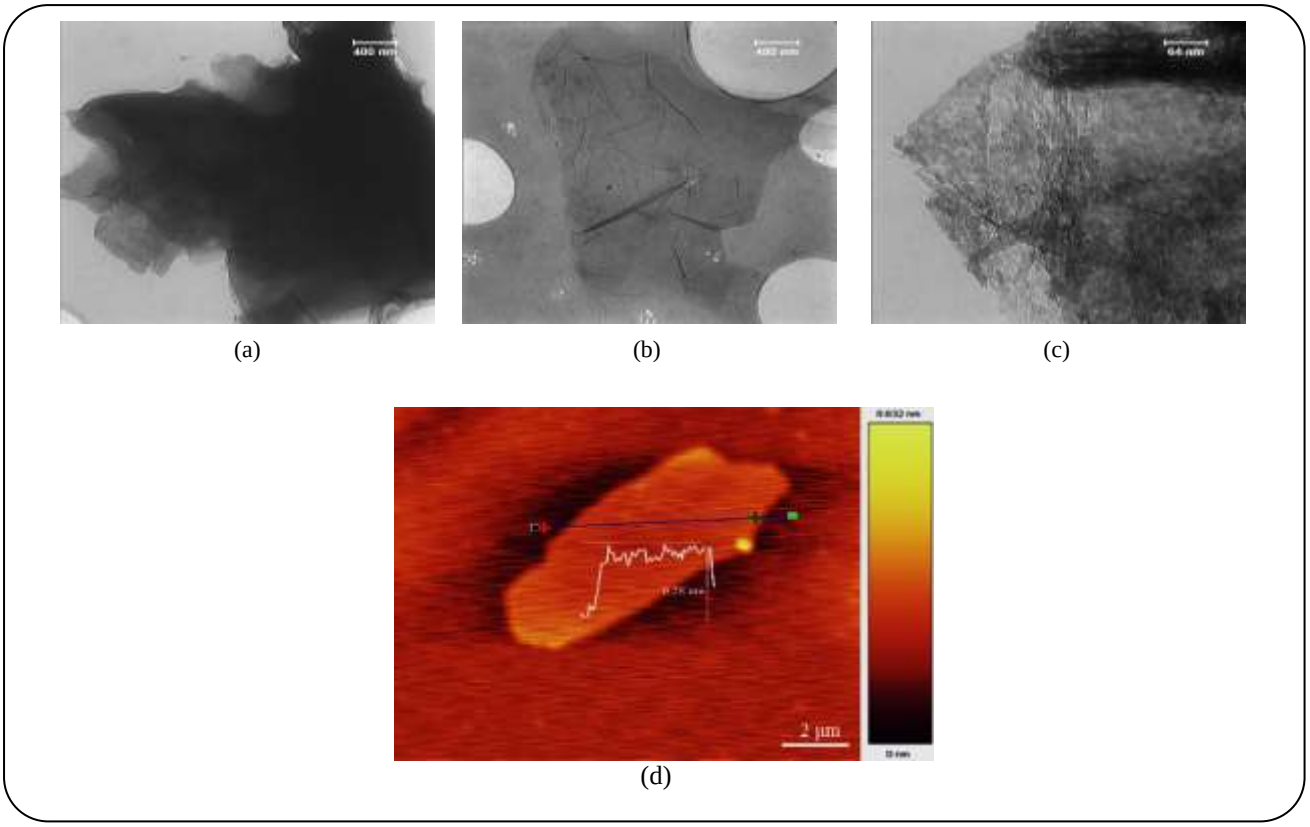

Fig. 2: TEM images of (a) graphite, (b) GO, (c) rGO@SiO_2, and (d) AFM image of the synthesized GO.

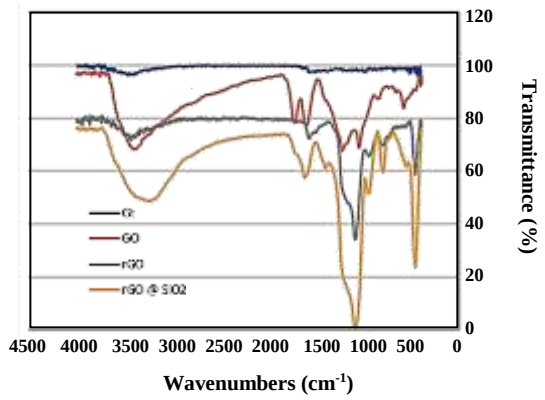

Fig. 3: FT-IR spectrum of the synthesized products.

2θ peak of the oxidized graphite is shifted to 2θ=10°, refers to interspace-expanding of the layers due to full carboxyl functionalization of nanosheets. The GO diffraction peak shifted to a lower diffraction angle than that observed for the graphite, confirming successful GO preparation achieved using the proposed modified Hummers method. However, after the preparation of rGO and rGO@SiO_2, the XRD pattern showed a typical broad peak of about $2\theta \approx 23°$ corresponding to the reduced GO planes [55].

The tensile stress-strain response of the elastomeric composites fabricated with and without the synthesized thin flakes is presented in Fig 5. The tensile stress of the blank, SBR is 0.28 MPa. An increase in tensile stress was observed for composites formulated by graphene (rGO) and rGO@SiO_2. For example, the tensile stress of polymer reinforced with 4 Phr of rGO and rGO@SiO_2 increased to 0.56 MPa and 0.50 MPa, which 2 and 1.78 times higher than the blank SBR, respectively. Other investigations about tensile elongation showed a decrease in elongation to failure with the incorporation of the filler, which is common for material composites. The behavior could be due to the improved interfacial interaction and suitable dispersion of the additives. The large surface area layer-like additives can strongly reinforce the stiffness and strength of SBR matrix, as a result, the tensile strain of the same additive-loaded polymers decreases [56]. Therefore, high-strength elastomer composites can be obtained with uniformly-dispersed graphene-based additives.

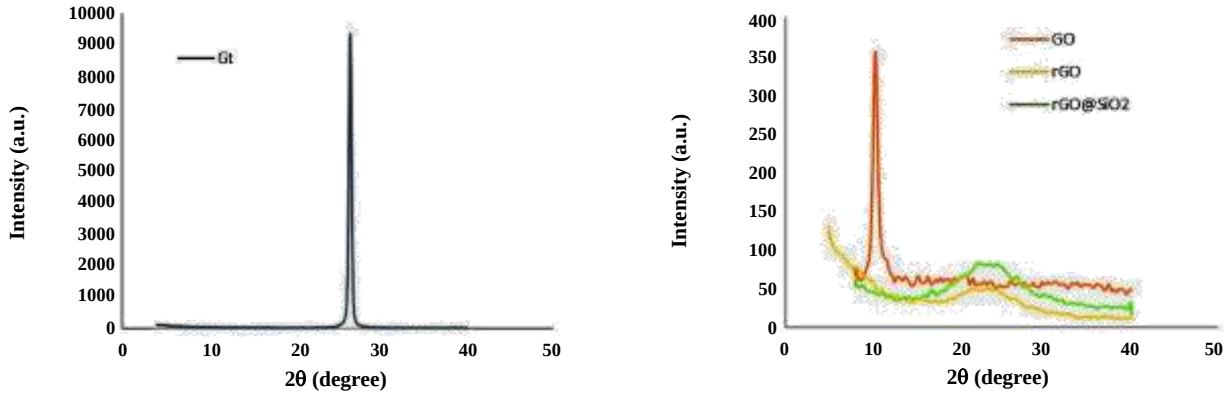

Fig. 4: XRD patterns of pristine graphite, synthesized GO and SiO_2@rGO.

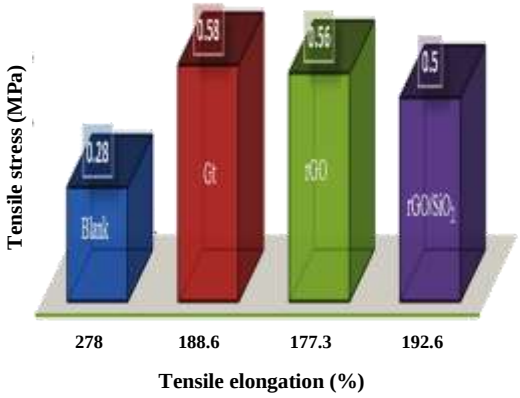

Fig. 5: Tensile stress and strain properties of the processed SBR and composites.

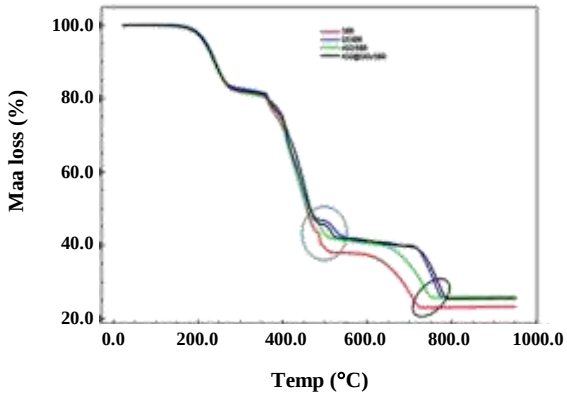

Fig. 6: TGA curves of the processed SBR-based compounds.

The TGA thermograph of SBR compound and the composite samples in an air atmosphere (Fig. 6) displayed multistep degradation under the heating rate of 10 ℃. The initial degradation of the manufactured SBR is at 175 ℃ which ends around 280 ℃. The weight loss at low temperatures can be due to some oligomers and intermediates involved in the composition [57]. At the degradation temperature of about 450-550 and 650-800 ℃, the weight loss percentage was decreased from 43.5 to 40 and 76.8 to 74.2 respectively, with the addition of the synthesized additives (4 phr). Increasing the thermal stability of the compounded products with the addition of large surface area additives could be attributed to the improvement in interfacial adhesion between the carbon-based layers and the elastomeric chain [56].

OIT is a sensitive method to determine the level of antioxidative additives within the polymer (e.g. rubbers), especially for those with unsaturated C-C bonds suffering from thermo-oxidative aging due to the integrated effects of heat and oxygen, which is the underlying process of materials degradation and of concern in various applications. Based on this, the antioxidative efficiency of the synthesized rGO and rGO@SiO_2 was evaluated by oxidation induction time (OIT) for elastomeric composites as shown in Fig. 7. Accordingly, Fig. 7a shows that the degradation of the neat SBR is faster than that of rGO/SBR and rGO@SiO_2/SBR but is slower than that of Gt/SBR compound. The OIT values of the neat SBR compound, Gt/SBR, rGO/SBR, and rGO@SiO_2/SBR were 30.46, 26.04, 44.33, and 39.85 min, respectively. The highest OIT values at 4 phr loading of rGO and rGO@SiO_2 were 1.45 and 1.3 times longer than that of neat SBR, respectively. It indicated that the thermal-oxidative stability of SBR was saliently improved with 4 phr loading of the thin materials.

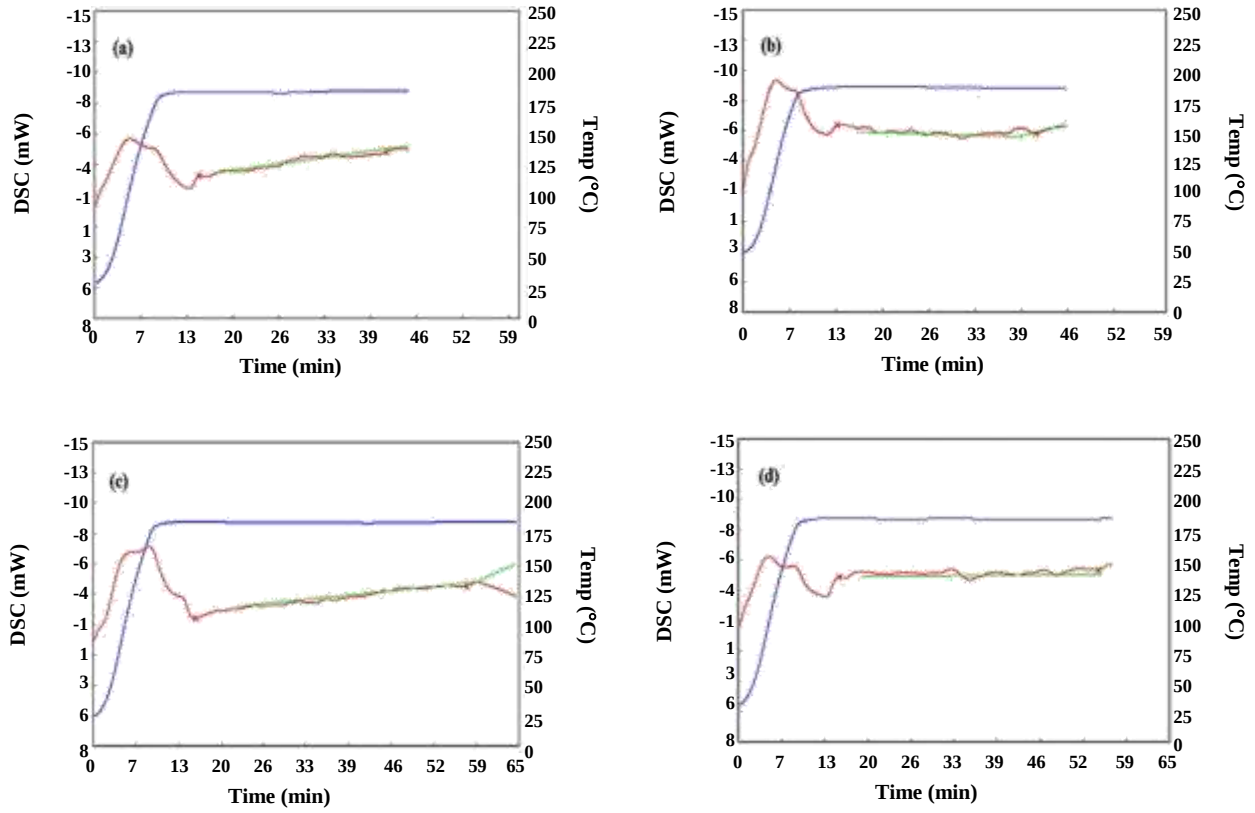

Fig. 7: DSC curves of the compounds for OIT study: (a) neat SBR (without additive), (b) SBR/graphite, (c) SBR/rGO, (d) SBR/rGO@SiO_2, (−: DSC as a function of time, −: temperature as a function of time, −: OIT).

High resistance to oxidative degradation of the modified SBR compound can be related to the fine dispersion of the synthesized additives in the polymer matrix [58]. Uneven distribution of block-like compressed layers of the graphite in the polymer chains can be one of the important reasons for the decrease in their oxidative resistance.

CONCLUSIONS

GO has been synthesized by a modified Hummers method from graphite powder. The synthesized GO was surface modified by TEOS to prepare SiO_2-coated rGO sheets. rGO was synthesized following an inexpensive one-step approach from pristine graphite, separately. Using the presented approaches have obtained a high yield and good quality of the GO, rGO@SiO_2, and rGO powders. Oxidation, reduction, and surface coating of the material's chemical structures were confirmed by XRD and FT-IR analyses. The separation of the compressed layers of the pristine graphite is confirmed with TEM image. The synthesized layer-like materials were successfully mechanically loaded into SBR matrix. The mechanical and thermal behavior of the compounded products so much has grown by adding only 4 phr of the synthesized materials. So, the tensile stress of the modified products increased virtually two times greater than the neat SBR. Loading of the reduced and modified GO showed much better thermal stability than blank SBR with excellent long-term thermo-oxidative aging resistance. Due to the unique properties of the synthesized and final processed products, these methods can provide a new approach of about GO preparation, its derivatives, and nanocomposites of elastomer/carbon-based materials. The elastomeric composites can apply to future various applications like electronic packaging and thermal management.

Acknowledgments

The authors gratefully acknowledge the financial support of the Ferdowsi University of Mashhad (project code:

3/47733), Mashhad, Iran, and the technical equipment and chemical support of Ayegh Khodro Toos (AKT) Co. of Part Lastic Industrial Group Co.

Received : Dec. 25, 2020 ; Accepted : Feb. 22, 2021

REFERENCES

[1] Huang C., Qian X., Yang R., Thermal Conductivity of Polymers and Polymer Nanocomposites, *Mater. Sci. Eng. R. Rep.*, **132**: 1-22 (2018).

[2] Agarwal S., Khan M.M.R., Gupta R.K., Thermal Conductivity of Polymer Nanocomposites made with Carbon Nanofibers, *Polym. Eng. Sci.* **48(12)**: 2474 - 2481 (2008).

[3] Mutiso R.M., Winey K.I., Electrical Properties of Polymer Nanocomposites Containing Rod-Like Nanofillers, *Prog. Polym. Sci.*, **40**: 63-84 (2015).

[4] Hu N., Masuda Z., Yan C., Yamamoto G., Fukunaga H., Hashida T., The Electrical Properties of Polymer Nanocomposites with Carbon Nanotube Fillers, *Nanotechnol.*, **19**:21 (2008).

[5] Buxton GA., Balazs AC., Predicting the Mechanical and Electrical Properties of Nanocomposites Formed from Polymer Blends and Nanorods, *Mol. Simul.*, **30(4)**: 249-257 (2004).

[6] Li S., Lin MM., Toprak MS., Kim DK., Muhammed M., Nanocomposites of Polymer and Inorganic Nanoparticles for Optical and Magnetic Applications, *Nano. Rev.*, **1**: 5214 (2010).

[7] Ross P., Escoba G., Sevilla G., Quagliano J., Micro and Nanocomposites of Polybutadienebased Polyurethane Liners with Mineral Fillers and Nanoclay: Thermal and Mechanical Properties, *Open. Chem.*, **15(1)**: 46–52 (2017).

[8] Rybiński P., Anyszka R., Imiela M., Siciński M., Gozdek T., Effect of Modified Graphene and Carbon Nanotubes on the Thermal Properties and Flammability of Elastomeric Materials, *J. Therm. Anal. Calorim.*, **127**: 2383–2396 (2017).

[9] Habeeb S. A., Al-Obad ZKM, and Albozahid M. A., Effect of Zinc Oxide Loading Levels on the Cure Characteristics, Mechanical and Aging Properties of The EPDM Rubber, *International Journal of Mechanical Engineering and Technology (IJMET).* **10**: 133-141 (2019).

[10] Habeeb S., Enhancing the Properties of Styrene-Butadiene Rubber by Adding Borax Particles of Different Sizes, *Iran. J. Chem. Chem. Eng.(IJCCE)*, **40(5)**: 1616-1629 (2021).

[11] Che J., Wu K., Lin Y., Wang K., Fu Q., Largely Improved Thermal Conductivity of HDPE/Expanded Graphite/Carbon Nanotubes Ternary Composites *via* Filler Network-Network Synergy, *Compos. Part. A. Appl. Sci. Manuf.*, **99**: 32-40 (2017).

[12] Lin S., A S Anwer M., Zhou Y., Sinha A., Carson L., Naguib H E., Evaluation of The Thermal, Mechanical and Dynamic Mechanical Characteristics of Modified Graphite Nanoplatelets and Graphene Oxide High-Density Polyethylene Composites, *Compos. B. Eng.*, **132**:61-68 (2018).

[13] Zhao Y H., Zhang Y F., Bai S L., Yuan X W., Carbon Fibre/Graphene Foam/Polymer Composites with Enhanced Mechanical and Thermal Properties, *Compos. B. Eng.*, **94**: 102-108 (2016).

[14] Liu Y., Zhang H., Porwal H., Tu W., Wan K., Evans J., Newton M., Busfield J J C., Peijs T., Bilotti E., Tailored Pyroresistive Performance and Flexibility by Introducing a Secondary Thermoplastic Elastomeric Phase into Graphene Nanoplatelet (GNP) Filled Polymer Composites for Self-Regulating Heating Devices, *J. Mater. Chem. C.*, **6(11)**: 2760-2768 (2018).

[15] Lee H B., Kim Y W., Yoon J., Lee N K., Park S H., 3D Customized and Flexible Tactile Sensor Using a Piezoelectric Nanofiber Mat and Sandwich-Molded Elastomer Sheets, *Smart Mater. Struct.*, **26**: 045032 (2017).

[16] Han J., Zhang X., Guo W., Wu C., Effect of Modified Carbon Black on the Filler–Elastomer Interaction and Dynamic Mechanical Properties of SBR Vulcanizates, *J. Appl. Polym. Sci.* **100(5)**:3707-3712 (2006).

[17] Du A., Wu M., Changyan S., Chen H., The Characterization of Pyrolytic Carbon Black Prepared from Used Tires and its Application in Styrene–Butadiene Rubber (SBR), *J. Macromol. Sci. B.* 47(2):268-275 (2008).

[18] Orton H., History of Underground Power Cables, *IEEE Electr. Insul. Mag.*, **29(4)**: 52-57 (2013).

[19] Yang Y., Zhang H., Zhang K., Liu L., Ji L., Liu Q., Vulcanization, Interfacial Interaction, and Dynamic Mechanical Properties of In-Situ Organic Amino Modified Kaolinite/SBR Nanocomposites Based on Latex Compounding Method, *Appl. Clay. Sci.*, **185**: 105366 (2020).

[20] Raslan H.A., El-Saied H.A., Mohamed R.M., Yousif N., Gamma Radiation Induced Fabrication of Styrene Butadiene Rubber/ Magnetite Nanocomposites for Positive Temperature Coefficient Thermistors Application, *Compos. B. Eng.*, **176**: 107326 (2019).

[21] Abraham J., Thomas J., Kalarikkal N., George S.C., Thomas S., Static and Dynamic Mechanical Characteristics of Ionic Liquid Modified MWCNT-SBR Composites: Theoretical Perspectives for the Nanoscale Reinforcement Mechanism, *J. Phys. Chem. B.*, **122(4)**: 1525-1536 (2018).

[22] Chen J., Wei H., Bao H., Jiang P., Huang X., Millefeuille-Inspired Thermally Conductive Polymer Nanocomposites with Overlapping BN Nanosheets for Thermal Management Applications, *ACS Appl. Mater. Interfaces.*, **11(34)**: 31402-31410 (2019).

[23] Chen J., Huang X., Zhu Y., Jiang P., Cellulose Nanofiber Supported 3D Interconnected BN Nanosheets for Epoxy Nanocomposites with Ultrahigh Thermal Management Capability, *Adv. Funct. Mater.*, **27(5)**: 1604754 (2016).

[24] Mohammed F.Q., Hasan A.S., Habeeb S.A., Bkeet W.G., Transport Properties and Applications of Graphene Nano-Ribbon-BN, *Test Engineering and Management.*, **83(1)**:10998-11002 (2020).

[25] Machrafi H., Lebon G., Iorio C S., Effect of Volume-Fraction Dependent Agglomeration of Nanoparticles on the Thermal Conductivity of Nanocomposites: Applications to Epoxy Resins, Filled by SiO_2, AlN and MgO Nanoparticles, *Compos. Sci. Technol.*, **130**:78-87 (2016).

[26] Mishra S.K., Shukla D.K., Patel R.K., Flexural Properties of Functionally Graded Epoxy-Alumina Polymer Nanocomposite, *Mater. Today.*, **5(2)**: 8431-8435 (2018).

[27] Choudhary S., Structural, Morphological, Thermal, Dielectric, and Electrical Properties of Alumina Nanoparticles Filled PVA–PVP Blend Matrix-Based Polymer Nanocomposites, *Polym. Compos.*, **39(S3)**: E1788-E1799 (2018).

[28] Zhang L., Deng H., Fu Q., Recent Progress on Thermal Conductive and Electrical Insulating Polymer Composites, *Compos. Commun.*, **8**: 74-82 (2018).

[29] Alva G., Lin Y., Fang G., Thermal and Electrical Characterization of Polymer/Ceramic Composites with Polyvinyl Butyral Matrix, *Mater. Chem. Phys.*, **205**:401-415 (2018).

[30] He J., Wang H., Su Z., Guo Y., Tian X., Qu Q., Linc Y. L., Thermal Conductivity and Electrical Insulation of Epoxy Composites with Graphene-SiC Nanowires and $BaTiO_3$, *Compos. Part. A. Appl. S.*, **117**: 287-298 (2019).

[31] Kim K., Ju H., Kim J., Vertical Particle Alignment of Boron Nitride and Silicon Carbide Binary Filler System for Thermal Conductivity Enhancement, *Compos. Sci. Technol.*, **123**: 99-105 (2016).

[32] Sun R., Yao H., Zhang H B., Li Y., Mai Y.W., Yu Z.Z., Decoration of Defect-Free Graphene Nanoplatelets with Alumina for Thermally Conductive and Electrically Insulating Epoxy Composites, *Compos. Sci. Technol.*, **137**:16-23 (2016).

[33] Guo S., Zheng R., Jiang J., Yu J., Dai K., Yan C., Enhanced Thermal Conductivity and Retained Electrical Insulation of Heat Spreader by Incorporating Alumina-Deposited Graphene Filler in Nano-Fibrillated Cellulose, *Compos. B. Eng.* **178**: 107489 (2019).

[34] Zhang L., Li X., Deng H., Jing Y., Fu Q., Enhanced Thermal Conductivity and Electrical Insulation Properties of Polymer Composites *via* Constructing Pglass/CNTs Confined Hybrid Fillers, *Compos. Part A Appl. Sci. Manuf.*, **115**: 1-7 (2018).

[35] Zifeng W., Chunyi Z., "Thermally Conductive Electrically Insulating Polymer Nanocomposites", Springer, Cham, Switzerland (2016).

[36] Papageorgiou D.G., Kinloch I.A., Young R.J., Graphene/Elastomer Nanocomposites, *Carbon.*, **95**: 460-484 (2015).

[37] Böhning M., Frasca D., Schulze D., Schartel B., "Multilayer Graphene/Elastomer Nanocomposites", Elsevier, London (2019).

[38] Habib N A., Chieng B W., Mazlan N., Rashid U., Yunus R., Rashid S A., Elastomeric Nanocomposite Based on Exfoliated Graphene Oxide and Its Characteristics Without Vulcanization, *J. Nanomater.*, **2017**: 1-11 (2017).

[39] Radadiya T., A Properties of Graphene, *Eur. J. Mater. Sci. Eng. (EJMS).*, **2**: 6-18 (2015).

[40] Zhen Z., Zhu H., "Structure and Properties of Graphene", Academic Press, Massachusetts (2018).

[41] Xu Z., "Fundamental Properties of Graphene", Academic Press, Massachusetts (2018).

[42] Lee B., Koo M.Y., Jin S.H., Kim K.T., Hong S.H., Simultaneous Strengthening and Toughening of Reduced Graphene Oxide/Alumina Composites Fabricated by Molecular-Level Mixing Process, *Carbon*, **78**: 212-219 (2014).

[43] Guo X., Xie K., Wang Y., Kang Z., Zhou W., Cheng S., Reduced Graphene Oxide -Coated 3D Interconnected SiO_2 Nanoparticles with Enhanced Lithium Storage Performance, *Int. J. Electrochem. Sci.*, **13**: 5645–5653 (2018).

[44] Pu X., Zhang H.B., Li X., Gui C., Yu Z Z., Thermally Conductive and Electrically Insulating Epoxy Nanocomposites with Silica-Coated Graphene, *RSC Adv.*, **4**: 15297-15303 (2014).

[45] Singh S., Rathi K., Pal K., Synthesis, Characterization of Graphene Oxide Wrapped Silicon Carbide for Excellent Mechanical and Damping Performance for Aerospace Application, *J. Alloys Compd.*, **740**: 436-445 (2018).

[46] Hsiao M.C., Ma C-C.M., Chiang J.C., Ho K.K., Chou T.Y., Xie X., Tsai C.H., Chang L.H., Hsieh C.K., Thermally Conductive and Electrically Insulating Epoxy Nanocomposites with Thermally Reduced Graphene Oxide-Silica Hybrid Nanosheets, *Nanoscale*, **5**: 5863–5871 (2013).

[47] Motagaly A.T., Rouby W.M., El-Sherbiny I.M., Farghalia A.A., El-Dek S., Fast Technique for the Purification of As-Prepared Graphene Oxide Suspension, *Diam. Relat. Mater.*, **86**: 20-28 (2018).

[48] Soltani T., Lee B K., Low Intensity-Ultrasonic Irradiation for Highly Efficient, Eco-Friendly and Fast Synthesis of Graphene Oxide, *Ultrason. Sonochem.*, **38**: 693-703 (2017).

[49] Abdolhosseinzadeh S., Asgharzadeh H., Kim H.S., Fast and Fully-Scalable Synthesis of Reduced Graphene Oxide, *Sci. Rep.*, **5**:1-7 (2015).

[50] Zhang S., Thuy Hang N., Zhang Z., Yue H., Yang W., Preparation of g-C_3N_4/Graphene Composite for Detecting NO_2 at Room Temperature, *Nanomaterials*., **7(1)**: 12 (2017).

[51] El-Badawy F.M., El-Desoky H.S., Quantification of Chloroxylenol, a Potent Antimicrobial Agent in Various Formulations and Water Samples: Environmental Friendly Electrochemical Sensor Based on Microwave Synthesis of Graphene, *J. Electrochem. Soc.*, **165(14)**: B694-B707 (2018).

[52] Wu H., Tang B., Wu P., Development of Novel SiO_2–GO Nanohybrid/Polysulfone Membrane with Enhanced Performance, *J. Membr. Sci.*, **451**: 94-102 (2014).

[53] Balaiah P., G.A., BD L., A Simple Approach to Stepwise Synthesis of Graphene Oxide, *J. Nanomed. Nanotechnol.*, **6(1)**: 1-4 (2015).

[54] Lee S.C., Some S., Kim S W., Kim S.J., Seo J., Lee J., Lee T., Ahn J-H., Choi H-J., Jun S.C., Efficient Direct Reduction of Graphene Oxide by Silicon Substrate, *Sci. Rep.*, **5**:1-9 (2015).

[55] Zhang X., Dong P., Zhang B., Tang S., Yang Z., Chen Y., Yang W., Preparation and Characterization of Reduced Graphene Oxide/Copper Composites Incorporated with Nano-SiO_2 Particles, *J. Alloys Compd.*, **671**: 465-472 (2016).

[56] Jasna V.C., Ramesan M.T., Fabrication of Novel Nanocomposites from Styrene-Butadiene Rubber/Zinc Sulphide Nanoparticles, *J. Mater. Sci.*, **53**: 8250–8262 (2018).

[57] Wang L., Hu L., Gao S., Zhao D., Zhang L., Wang W., Bio-Inspired Polydopamine-Coated Clay and its Thermo-Oxidative Stabilization Mechanism for Styrene Butadiene Rubber, *RSC Adv.*, **5**: 9314-9324 (2015).

[58] Zhong B., Dong H., Luo Y., Zhang D., Jia Z., Jia D., Liu F., Simultaneous Reduction and Functionalization of Graphene Oxide *via* Antioxidant for Highly Aging Resistant and Thermal Conductive Elastomer Composites, *Compos. Sci. Technol.* **151**: 156-163 (2017).